

## Time-Dependent Density-Functional Calculations of Field Emissions from Carbon Allotropes

K. Watanabe<sup>1,2</sup> M. Araidai<sup>1,2</sup> K. Tada<sup>3</sup> and A. Yamauchi<sup>4</sup>

<sup>1</sup>Department of Physics, Tokyo University of Science, 1-3 Kagurazaka, Shinjuku-ku, Tokyo 162-8601, Japan  
Fax: 81-3-3260-4665, e-mail: kazuyuki@rs.kagu.tus.ac.jp

<sup>2</sup>Core Research for Evolutional Science and Technology (CREST), Japan Science and Technology Agency, 4-1-8 Honmachi, Kawaguchi, Saitama 332-0012, Japan

<sup>3</sup>Geosphere Environmental Technology Corporation, 1-26-5 Toranomon, Minato-ku, Tokyo 105-0001, Japan

<sup>4</sup>Information and Telecommunication Systems, Hitachi Ltd., Hitachi Systemplaza Shin-Kawasaki, 890 Kashimada, Saiwai, Kawasaki, Kanagawa 212-8567, Japan

We apply time-dependent density-functional theory to field emission of carbon allotropes. The electronic states origin of field emission properties reflecting the atomic geometries and hydrogen termination of edges are elucidated through the analysis of energy band structures, energy distribution of emitted electrons, and  $\sigma$ - and  $\pi$ -bonding natures. Findings in this study provide the theoretical basis for understanding the FE mechanism of covalent-bond materials and designing Si- and C-based nanostructured field emitters.

Key words: Field emission, Time-dependent density-functional theory, Carbon allotrope, Electronic structures

### 1. INTRODUCTION

Understanding electronic transport phenomena in nano-scale materials is a challenge for theoretical studies, because materials-dependent quantum simulation methods suitable for treating such nonequilibrium electron dynamics are prerequisite to provide a theoretical basis to elucidate the microscopic origin. Recently, we have successfully applied the time-dependent density-functional theory (TD-DFT)[1-3] to electron field-emission (FE) of some carbon materials.[4-6] The TD-DFT within a real-time scheme is a powerful method for treating field-induced electron tunneling which is a typical nonequilibrium electron dynamics and determining the FE current.

Field emissions (FE) of various systems have been extensively studied both experimentally and theoretically for a long time. Among these, diamond has been expected to be one of the promising candidates for an ideal field emitter[7] because of negative electron affinity[8] in addition to its superior properties such as chemical inertness, mechanical hardness and low threshold voltage. Thus far, a number of possible mechanisms to interpret the observed emission properties of diamond surfaces have been proposed. In particular, attention should be paid to the experiment performed by Bandis and Pate; they show that field-emitted electrons are from the valence band rather than the conduction band of boron-doped diamond.[9] The microscopic mechanism of field emission of diamond surfaces, however, remains to be clarified.

Recently, carbon nanotube field emitters[10-13] are predicted as an application to next-generation flat-panel displays because CNTs have intrinsically suitable properties for field emitters, such as high aspect ratio, high mechanical stiffness, chemical inertness and electrical conductivity. Experimentally, highly enhanced FE currents have been observed for open-ended

multi-walled carbon nanotubes (MWNTs) and the cause has been attributed to emissions from an atomic chain unraveling from the edge of the nanotubes.[14] Recently, pentagonal shapes have been observed by field emission microscopy (FEM) of capped MWNTs.[15] However, the emission mechanism of CNTs is not understood and these unusual phenomena in FE from CNTs remain to be explained.

Theoretically, the Fowler-Nordheim (F-N) theory based on the free electron model[16] has been useful for explaining the current-voltage characteristics in the experiments on FE of usual micron-sized metallic tips. However, any quantitative arguments based on the F-N theory are highly questionable especially for the analysis of the FE characteristics unique to covalent-bond nanostructures including carbon allotropes and related materials.

In this review, we describe the results of FE of a carbon atom, silicon clusters,[4] graphitic ribbons[5] and diamond surfaces.[6] based on the TD-DFT calculations focusing on the electronic states origin of FE of covalent-bond materials.

### 2. METHOD

The present method is based on the conventional density-functional theory (DFT) [17] to determine the electronic states and the time-dependent density-functional theory (TD-DFT) [1,18] to evaluate FE current under an electric field. We used the generalized gradient approximation (GGA) for the exchange-correlation potential[19] and the norm-conserving pseudopotentials of NCPS97[20] based on the Troullier-Martins algorithm[21]. We expand the electronic wave functions in plane waves up to a kinetic energies of 39.5 Ry for a carbon atom and 14.2 Ry for silicon clusters. The cutoff kinetic energy of 44 Ry is used for graphitic ribbons and diamond surfaces. The unit cells of rectangular box including vacuum regions

with the dimensions of  $105.8 \text{ \AA} (x) \times 10.6 \text{ \AA} (y) \times 10.6 \text{ \AA} (z)$ ,  $79.8 \text{ \AA} \times 2.49 \text{ \AA} \times 4.99 \text{ \AA}$ ,  $76.8 \text{ \AA} \times 4.32 \text{ \AA} \times 4.32 \text{ \AA}$  and  $101 \text{ \AA} \times 5.03 \text{ \AA} \times 2.52 \text{ \AA}$  are used for clusters, zigzag graphitic ribbons, armchair graphitic ribbons, and diamond surfaces, respectively. An electric field is applied to these systems in the direction of  $x$ . For  $k$  point samplings in the Brillouin zones,  $\Gamma$  point is chosen for clusters, eleven points along the ribbon axis for graphitic ribbons and six points for diamond surfaces.

In the calculation of the time evolution of wave functions in the TD-DFT algorithm, both the Suzuki-Trotter split operator method[2,22] and the fifth-order Taylor expansion method[1] were used. Since the difference in the FE currents obtained by the two methods is negligible and the latter method guarantees the normalization condition on the electron number within an accuracy of  $10^{-7}$  for simulation time  $t \sim 100$  a.u. (2.4fs), we employed the latter scheme to save computational time in this study. The time step for the integration is 0.05a.u. After optimizing the electronic states of the systems under no electric field, the electric field is switched on and increased to  $\sim 10$  V/nm linearly until  $t = 25$  a.u. Finally, the value of the FE current is evaluated from the linear slope of the curve of the number of emitted electrons as a function of time.

### 3. RESULTS

#### 3.1 Field emission of atomic clusters

First, we evaluate the emission currents under an electric field of 2 V/nm for Si and C atoms (*i.e.*, field ionization) and the values obtained are 45 nA and 6 nA, respectively. This is physically reasonable because the energy of highest occupied atomic orbital from the vacuum level (corresponds to work function for bulk metals) is lower for Si (4.2eV) than for C (5.4eV).

Here, we describe the results on FE currents from  $\text{Si}_n$  ( $n=1-4$ ) clusters in Fig.1. The currents emitted from the  $\text{Si}_n$  clusters and the current components from each molecular electronic states of clusters (from the right to left of  $\text{Si}_n$ ) are for the states from higher to lower in energy) are indicated by thick bars and thin bars, respectively. The numbers refer the total emission currents from the clusters in units of nA. The  $\sigma$ -bonding states are indicated by " $\sigma$ ". The total emission current increases as  $n$  increases. This feature, however, cannot be understood by a conventional formula of emission current, because the highest-occupied-molecular-orbital (HOMO) energy from the vacuum level (defined as  $\delta E_H$  in this paper) increases as  $n$  increases.[4] The main cause to govern the property is found to reside in the  $\sigma$  nature of the main level. All the levels that emit the highest current for each cluster have the  $\sigma$ -bonding nature. Further, the electron density of the  $\sigma$  state protrudes more from the tip of molecular chain for longer (larger  $n$ ) clusters. This is the reason why the emission current *increases* as  $n$  increases despite the *increase* in  $\delta E_H$ . We also understand by noticing the important role of the  $\sigma$  orbitals that the HOMO is not necessarily the major contributor to FE.[4]

We describe the local electronic structures of  $\text{Si}_4$  cluster to clarify the role of the  $\sigma$ -orbital state in FE.

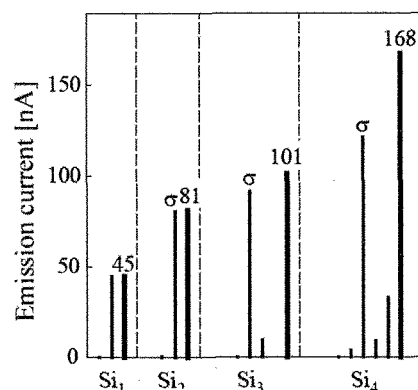


Fig. 1 Emission currents from molecular levels of valence electrons of  $\text{Si}_n$  ( $n=1-4$ ) clusters in an electric field of 2V/nm. The height of the bars from right to left of  $\text{Si}_n$  refers the emission current from the levels of the highest (HOMO) to lower levels of  $\text{Si}_n$ . The thick bars on the right for each cluster indicate the total emission current from the clusters. The numbers give the current in units of nA.  $\sigma$  indicates the  $\sigma$ -bonding states.

We draw the electron-density distributions of the three major emitted-levels of  $\text{Si}_4$  on the plane of the cluster axis in Fig. 2. The electric field is applied along the cluster axis and the electron is emitted toward the upper vacuum. It is evidently seen from Fig. 2 that the HOMO (left panel) and the second highest level (center panel) have  $\pi$  nature, and the third highest level (right panel) that emits the highest current has  $\sigma$  nature. The  $\sigma$  bond is found to have the electron density highly protruding from the top silicon atom toward the vacuum by comparing with the  $\pi$  distributions of the left and center panels. This means that the states with higher electron-distribution in the direction of electric field generate more emission-currents.

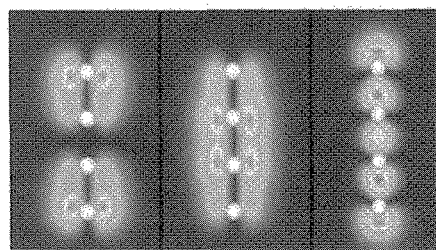


Fig.2 Electron-density distributions of the molecular energy levels of  $\text{Si}_4$  on the plane of the cluster axis including silicon atoms (spheres). The electron distributions on the left, center and right panels are for the HOMO, second and third highest levels given in Fig. 1. The  $\pi$  character is seen on the left and center panels and the  $\sigma$  character on the right panel.

#### 3.2 Field emission of graphitic ribbons

The band structures as a function of wave number  $k_y$  are shown for the clean zigzag ribbon (without hydrogen (H) termination) in Fig. 3(a) and for the H-terminated zigzag ribbon in Fig. 3(b). The edge state, which has been discussed in detail by Nakada *et al.*[23] is seen above the Fermi level in Fig. 3(a) and on the Fermi level in Fig. 3(b) near X points.

There are two important findings regarding the result on FE current from the clean and H-terminated zigzag ribbons. One is that the FE current from the clean zigzag

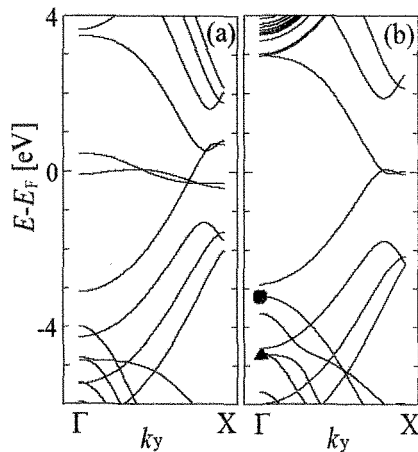


Fig.3 Band structures of (a) a clean zigzag ribbon and (a) H-terminated zigzag ribbon as a function of wave number  $k_y$ .

ribbon is larger than that from the H-terminated zigzag ribbon. The dominant part of the FE current from the clean zigzag ribbon comes from the dangling-bond states at the Fermi level (Fig. 3(a)). The dangling-bond states do not exist in the H-terminated zigzag ribbon but the  $\pi$  state remains (Fig. 3(b)). Since localized states such as dangling-bond states were found to significantly react with the electric field from the previous studies,[24-26] the present result enables us to confirm that the dangling-bond states essentially contribute to FE from clean graphitic ribbons.

The other important property is that the current decreases as  $k_y$  increases from  $\Gamma$  to X points. This feature initially appears to contradict the dispersions of the occupied band in Fig. 3(b). Here, we recall that the kinetic energy of electrons in the direction of the applied field is essentially responsible for electron tunneling into the vacuum.[16] Therefore, we define the energy eigenvalue,  $\varepsilon_x^i(k_y)$ [15] as

$$\varepsilon_x^i(k_y) = \langle \phi_{k_y}^i | d/dx^2 + v_{\text{eff}} | \phi_{k_y}^i \rangle \quad (1)$$

where  $i$  is the band index,  $\phi_{k_y}^i$  the wave function and  $v_{\text{eff}}$  the effective potential of the Kohn-Sham Hamiltonian.[17]  $\varepsilon_x^i$  has a larger value at the  $\Gamma$  point than at the X point, indicating that the tunneling probability of electrons is higher from the former point than the latter one. As a result, electron emissions from the *edge state* do not occur even though it is on the Fermi level.

The currents emitted from two zigzag ribbons in an electric field of 10V/nm are presented as a function of energy in Fig. 4. A large peak at the Fermi level of the clean zigzag ribbon (solid line) in Fig. 4 comes from the dangling-bond states in Fig. 3(a). On the other hand, the highest and second highest peaks of the H-terminated zigzag ribbon (broken line) come mainly from the states marked by a dot and a triangle at the  $\Gamma$  point in Fig. 3(b). These properties of the energy distribution also appear in armchair ribbons. The FE current is influenced much more by the condition of the edges, *i.e.*, clean or H-terminated, than by the structural difference, *i.e.*, zigzag or armchair type. We estimate the FE current

from a circular edge of graphitic sheet with  $\sim 1$ nm diameter of an open-ended MWNT under a high field of  $\sim 10$  V/nm to be  $\sim 1$   $\mu$ A, if the edge structure of graphitic sheets of an open-ended MWNT is regarded to be approximately the same as that of the graphitic ribbons. The order of magnitude of the result is compatible with the observed results.[13] The emission current is not expected to monotonically increase above  $\sim 1$   $\mu$ A as the tube diameter increases (a few tens of nm), because the field enhancement at the edge of nanotube decreases as the aspect ratio decreases.[27]

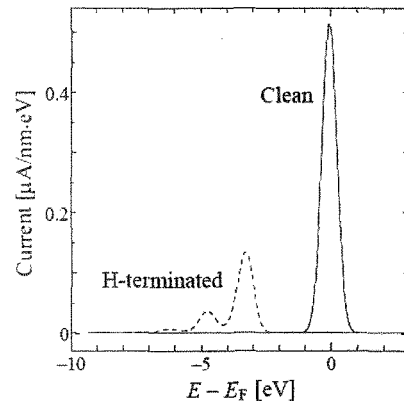


Fig. 4 Energy distribution of electrons emitted from a zigzag ribbon in a field of 10 V/nm.

### 3.3 Field emission of diamond surfaces

The electronic band structures of the clean and H-terminated diamond C(100)- $2 \times 1$  surfaces are given in Fig. 5. The dangling-bond (DB) states of the clean surface appear in the energy gap in Fig. 5(a). The DB states disappear upon H termination as seen in Fig. 5(b). The dispersions of the valence bands and the lower dangling-bond state that influence the FE characteristics are well compatible with those of a reliable *ab initio* calculation.[28] Since the previous studies have reported that the DB states are reactive to electric fields [5,26,29], the DB states are predicted to significantly contribute to FE. We evaluate the energy,  $\delta E_n$  of the occupied band  $n$  measured from the vacuum level of the clean and H-terminated diamond surfaces. The highest occupied state is the lower DB state in Fig. 5(a) and the  $\delta E_n$  is 5.70 eV for the clean surface. The DB states disappear and the  $\delta E_n$  of the valence band maximum is decreased to 3.98 eV upon H termination. We obtain the FE currents of 173 nA/nm<sup>2</sup> from the clean surface and 434 nA/nm<sup>2</sup> from the H-terminated surface under an electric field of 5 V/nm. The results mean that a higher FE current is predicted from the surface with a lower  $\delta E_n$ . This property of H termination on FE current from diamond surfaces has been already observed in experiments [7], although the direct comparison of the absolute values with the experimental ones cannot be made, because the ideal flat surfaces without any imperfections and protrusions, that cannot exist under usual experimental conditions, are assumed in the calculations.

Let's see the electronic states origin of the energy distribution of FE current density in Fig. 6. The panels

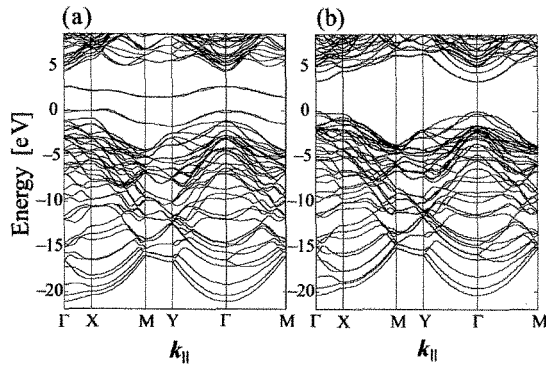


Fig. 5 Electronic band structures of (a) a clean and (b) an H-terminated C(100)-2 $\times$ 1 diamond surfaces.

(a) and (b) of Fig. 6 give the results for the clean and H-terminated surfaces, respectively. The electron distributions that are the source of current peaks are shown on the right side of each panel. A sharp peak in Fig. 6(a) originates from the two DB states (the  $\delta E_n$ s are 5.70 eV and 5.98 eV) which are localized at surfaces as seen in the electron distributions. On the other hand, two peaks appear for the H-terminated surface in Fig. 6(b). The lower peak comes from a localized surface state just below the dimer atoms. Unexpectedly, the higher peak is found not to originate from the surface state but from the bulk or inner state as evidently seen in the electron distribution. Further, the value of the highest peak is twice as large as that of the peak in Fig.6(a). Therefore, one should note that even *inner*

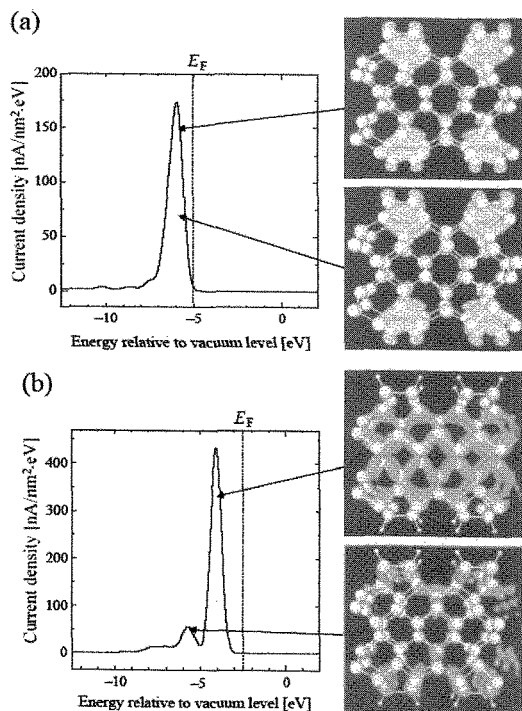


Fig. 6 Energy distributions of FE current densities of (a) a clean and (b) an H-terminated surfaces. On the right side of each panel, the electron distributions of  $\Gamma$  point causing the peaks are drawn by gray clouds with carbon atoms (white spheres) and hydrogen atoms (white dots) in the diamond slabs.

states can contribute to FE when the ionization energy is small enough for electron tunneling into the vacuum. More details about the electronic states origin of the current peaks in Fig. 6 have been discussed in the previous study[6] using  $\epsilon_x^i$  given in eq. (1), which is a measure of electron-density amplitude of the state  $i$  along the direction of FE.

#### 4. CONCLUSION

We present in this study that the time-dependent density-functional theory (TD-DFT) calculations are very adequate method for investigating the field emission (FE) of carbon-related nanostructures and revealing the electronic states origin of FE mechanism. The dangling-bond ( $\sigma$ ) states localized at edges or surfaces are main source of the FE current, which is a common property of covalent-bond structures. Hydrogen (H) termination effect on FE current, however, differs between graphitic ribbons and diamond surfaces due to the different atomic geometries of the edge and the surface. In marked contrast to FE of usual micron-sized metallic tips, local electronic states rather than work functions are found to be very crucial to understanding the FE mechanism of carbon nanostructures by using a quantity of energy eigenvalue in the direction of FE.

We believe these findings provide the theoretical basis for understanding and designing carbon-based nanostructured field emitters.

#### Acknowledgments

The authors thank H. Fujita and S. Watanabe for collaboration and stimulating discussions. The present study was partially supported by Ministry of Education, Sports, Culture, Science and Technology of Japan through the Grant-in-Aid No. 15607018. M. A. and K. T. thank the Supercomputer Center, Institute for Solid State Physics, University of Tokyo and the Computer Center, Information Technology Center, University of Tokyo for the use of their facilities.

#### References

- [1] K. Yabana and G.F. Bertsch: Phys. Rev. B 54, 4484 (1996).
- [2] O. Sugino and Y. Miyamoto: Phys. Rev. B 59, 2579 (1999).
- [3] N. Watanabe and M. Tukada: Phys. Rev. E 65, 036705 (2002).
- [4] M. Araidai, A. Yamauchi, and K. Watanabe, Jpn. J. Appl. Phys., in press.
- [5] K. Tada and K. Watanabe, Phys. Rev. Lett. 88 (2002) 127601.
- [6] M. Araidai and K. Watanabe, Jpn. J. Appl. Phys. 42, L666 (2003).
- [7] J.B. Cui and J. Robertson: J. Vac. Sci. Technol. B 20, 238 (2002).
- [8] J.van der Weide, Z. Zhang, P.K. Baumann, M.G. Wensell, J. Bernholc and R.J. Nemanich: Phys. Rev. B 50, 5803 (1994).
- [9] C. Bandis and B. B. Pate: Appl. Phys. Lett. 69, 366 (1996).
- [10] W.A.de Heer, A. Chatelain, D. Ugarte, Science 270, 1179 (1995).
- [11] Y. Saito, K. Hamaguchi, K. Hata, K. Uchida, Y.

- Tasaka, F. Ikazaki, M. Yumura, A. Kasuya and Y. Nishina, *Nature* 389, 554 (1997).
- [12] W.B. Choi, D.S. Chung, J.H. Kang, H.Y. Kim, Y.W. Jin, I.T. Han, Y.H. Lee, L.E. Jung, N.S. Lee, G.S. Park, and J.M. Kim, *Appl. Phys. Lett.* 75, 3129 (1999).
- [13] Y. Saito and S. Uemura, *Carbon* 38, 169 (2000).
- [14] A.G. Rinzler, J.H. Hafner, P. Nikolaev, L. Lou, S.G. Kim, D. Tomanek, P. Nordlander, D.T. Colbert, and R.E. Smalley, *Science* 269, 1550 (1995).
- [15] Y. Saito, K. Hata, and T. Murata, *Jpn. J. Appl. Phys.* 39, L271 (2000).
- [16] R. Gomer, *Field Emission and Field Ionization* (American Institute of Physics, New York, 1993).
- [17] W. Kohn and L.J. Sham, *Phys. Rev.* 140, A1133 (1965).
- [18] E. Runge and E.K.U. Gross, *Phys. Rev. Lett.* 52, 997 (1984).
- [19] J.P. Perdew, J.A. Chevary, S.H. Vosko, K.A. Jackson, M.R. Pederson, D.J. Singh, and C. Fiolhais, *Phys. Rev. B* 46, 6671 (1992).
- [20] K. Kobayashi, *Comput. Mater. Sci.* 14, 72 (1999).
- [21] N. Troullier and J.L. Martins, *Phys. Rev. B* 43, 199 (1991).
- [22] M. Suzuki, *J. Phys. Soc. Jpn.* 61, L3015 (1992).
- [23] K. Nakada, M. Fujita, G. Dresselhaus, and M. S. Dresselhaus, *Phys. Rev. B* 54, 17954 (1996).
- [24] S. Han and J. Ihm, *Phys. Rev. B* 61, 9986 (2000).
- [25] G. Zhou, W. Duan and B. Gu, *Phys. Rev. Lett.* 87, 095504 (2001).
- [26] K. Tada and K. Watanabe: *Jpn. J. Appl. Phys.* 39, 268 (2000).
- [27] A. Maiti, C.J. Brabec, C. Roland and J. Bernholc, *Phys. Rev. B* 52, 14850 (1995).
- [28] J. Furthmuller, J. Hafner, and G. Kresse: *Phys. Rev.* 53, 7334 (1996).
- [29] S. Han and J. Ihm: *Phys. Rev. B* 66 (2002) 241402(R).

(Received October 13, 2003; Accepted April 24, 2004)